Electrochemical Studies of Microbiologically Influenced Corrosion on API 5L X65 by Sulfate-Reducing Bacteria in CO_2 Environments

Zulkafli, Rabiahtul
Department of Applied Physics, Faculty of Science and Technology, Universiti Kebangsaan Malaysia

Norinsan Kamil Othman
Department of Applied Physics, Faculty of Science and Technology, Universiti Kebangsaan Malaysia

Yaakob, Najmiddin
Centre of Industrial Process Reliability and Sustainability (INPRES), Faculty of Chemical Engineering, Universiti Teknologi MARA

Fathul Karim Sahrani
Department of Earth Sciences and Environment, Faculty of Science and Technology, Universiti Kebangsaan Malaysia

他

https://doi.org/10.5109/6782167

出版情報：Evergreen. 10 (1), pp.601-607, 2023-03. 九州大学グリーンテクノロジー研究教育センター
バージョン：

Electrochemical Studies of Microbiologically Influenced Corrosion on API 5L X65 by Sulfate-Reducing Bacteria in CO_2 Environments

Rabiahtul Zulkafli[1], Norinsan Kamil Othman[1*], Najmiddin Yaakob[2], Fathul Karim Sahrani[3], M.S.H Al-Furjan[4]

[1]Department of Applied Physics, Faculty of Science and Technology, Universiti Kebangsaan Malaysia, 43600, Bangi, Selangor, Malaysia

[2]Centre of Industrial Process Reliability and Sustainability (INPRES), Faculty of Chemical Engineering, Universiti Teknologi MARA, 40450, Shah Alam, Selangor, Malaysia

[3]Department of Earth Sciences and Environment, Faculty of Science and Technology, Universiti Kebangsaan Malaysia, 43600, Bangi, Selangor, Malaysia

[4]School of Mechanical Engineering, Hangzhou Dianzi University, Hangzhou 310018, China

*E-mail: insan@ukm.edu.my

(Received December 8, 2021; Revised February 23, 2023; accepted February 23, 2023).

Abstract: The current study explores microbiologically influenced corrosion (MIC) of carbon steel API 5L X65 with and without the presence of sulfate-reducing bacteria (SRB) in CO_2 environments. The Electrochemical Impedance Spectroscopy (EIS), potentiodynamic polarisation and Field Emission Scanning Electron Microscopy (FESEM) techniques were employed to analyse the carbon steel's corrosion behaviour. The R_p values from the EIS signify lower values denoting the steel's greater corrosion rate. FESEM micrographs found a uniform corrosion on specimens without SRB whereas a pitting corrosion on specimens with SRB. The study concludes that SRB accelerate the corrosion progression due to MIC.

Keywords: CO_2 environments; oil and gas; pipeline corrosion; surface morphology

1. Introduction

Oil and gas carry a portion of water with varying volumes of gases and acids; both gases of carbon dioxide (CO_2) and hydrogen sulphide (H_2S) are the most common[1)]. According to the Natural Gas Industry Annual Review 2017, Malaysia faces a high CO_2 gas presence. In 2011, the global average atmospheric CO_2 reached 390.4 ppm surpassing the 390 ppm limit for the first time[2)]. Following the excess in CO_2 and H_2S, a worldwide threat is impending, particularly the environment[3–6)]. These conditions are detrimental to the service life and functionality of carbon steel[7)]. The inquiry on carbon dioxide corrosion, also known as sweet corrosion, especially on corrosion resistance of carbon steel, has piqued the interest of numerous researchers since the 70s. Steel degradation with carbon dioxide corrosion as the primary culprit has caused significant consequences for the oil and gas industries[8)].

The pervasive presence of microorganisms in several conditions such as oilfield water formation, oilfield water production, seawater and cooling water has initiated the MIC phenomenon (microbiologically influenced corrosion)[9)]. The anaerobic sulfate-reducing bacteria (SRB) are typically found in oilfields involving MIC pipelines[10)]. MIC materialises after the production of a biofilm on the surface of the steel[11,12)]. In the course of SRB's metabolic activity, reduction of sulfate ions occurs into three forms of sulfide ions, namely H_2S (soluble), HS^- and S^{2-} [13,14)]. The company of carbon dioxide (CO_2), hydrogen sulphide (H_2S), seawater and other particles initiate critical corrosion-related problems in oil and gas pipelines.

Research on MIC involving SRB in CO_2 environments are still lacking, especially in the Malaysian context. Researchers continue to explore mechanisms and electrochemical sequences for pitting corrosion in these environments. Hence, this paper seeks to study, through the exploitation of destructive and non-destructive electrochemical methods, the co-presence effects of SRB in CO_2 environments on the corrosion behaviour of API 5L X65.

2. Materials and experimental procedure

2.1 Microorganisms and culture

The samples of bacteria were obtained from local crude oil located in Melaka, Malaysia. This study utilises stock cultures that went through isolation and stored in semi-anaerobic conditions at −18°C. The stock cultures, consisting of two single bacteria of SRB (*Desulfococcy multivorans* and *Disulfovibrio sp.*), were employed to study corrosion on carbon steel in CO_2 environments. The SRB were cultured in an enrichment medium known as a VMNI medium. The medium was incubated for three full days at a maintained temperature of 30°C. Subsequently, the SRB were centrifuged at 3500 rpm for five minutes before being used in electrochemical measurements[15].

2.2 Culture medium

According to Zinkevich et al.[16], the VMNI medium is an enrichment medium prepared specifically for culturing SRB in the laboratory. The medium compositions employed were (g/L): 0.5 KH_2PO_4, 1.0 NH_4Cl, 4.5 Na_2SO_4, 0.3 $Na_3C_6H_5O_7$, 0.04 $CaCl_2.6H_2O$, 0.06 $MgSO_4.7H_2O$, 2.0 casamino acid, 2.0 tryptone, 5.0 sodium lactate, 0.1 ascorbic acid, 0.1 thioglycolic acid, 0.5 $FeSO_4.7H_2O$ and 1.0 yeast extract. The VMNI solution was prepared using filtered seawater. The pH of the solution was then set to 7.2 ± 0.1 using 1 M NaOH. Subsequently, at 121°C for 15 minutes, this VMNI medium was autoclaved before adding 1.0 mL trace elements and 2.0 mL vitamins at room temperature.

2.3 Metal samples preparation

The API 5L X65 carbon steel pipe were cut into coupons with elemental compositions (wt%), C: 0.16, Si: 0.45, Mn: 1.65, P: 0.020, S: 0.01, V: 0.09, Nb: 0.05 and Ti: 0.06. The coupons were machined into cuboid shapes with dimensions 10 mm x 20 mm x 2 mm. Later, a mould of non-conducting epoxy resin was prepared to embed the cuboid coupons and leaving an exposed area of 100 mm^2. Each coupon was soldered with a copper wire to establish an electrical connection. The cuboid-shaped coupons without mould in epoxy were used for biofilm growth. All the coupons were grind using grit silicon carbide papers of 600, 800 and 1200, and immersed in an acetone solvent for degreasing. Subsequently, the coupons were cleaned using anhydrous ethanol, dried and kept in a desiccator. Before testing, the coupons were sanitised under a UV lamp for 30 minutes[11].

2.4 Surface analysis of coupons exposed to bacteria

The Field Emission Scanning Electron Microscope (FESEM) technique carried out the surface analyses. In observing the biofilm production on the steel surface, the API 5L X65 coupons were incubated in a test solution containing SRB for 72 hours. The preparation of biological samples was done by soaking the coupons in 2.5 % glutaraldehyde solution for eight hours and dehydrated using series of ethanol[11]. Next, to amplify the electrical conductivity, the specimen's surface was coated with a thin gold film. In order to monitor the morphology of corrosion, the product was removed as per the guideline provided in the ASTM-G1-03 standards.

2.5 Bacteria cell counts

The SRB cell counts – which determines the growth process of SRB – were measured using Colony-Forming Unit (CFU) techniques by exposing the bacteria in VMNI medium to CO_2 for 30 days at 30°C. Fig. 1 shows a schematic diagram of the dilution factors to measure the numbers of bacteria formed in CO_2 environments. The dilution of bacterial samples was performed on certain days by extracting 1.0 mL of bacterial culture using a micropipette and dissolved in 9.0. mL of sterile seawater. This step was repeated for up to 7 to 10 dilution factors depending on the cell growth calculated on the VMNI agar plate. 0.1 mL of shaken solution was extracted using a micropipette, dropped, and spread on the agar plate for each dilution step. The agar plate was incubated in an anaerobic flask for 24–48 hours at 30°C. The numbers of colonies formed were calculated using the formula[17]:

$$\frac{CFU}{ml} = \frac{numbers\ of\ colony}{volume\ plated\ (ml)}\ x\ dilution\ factors \qquad (1)$$

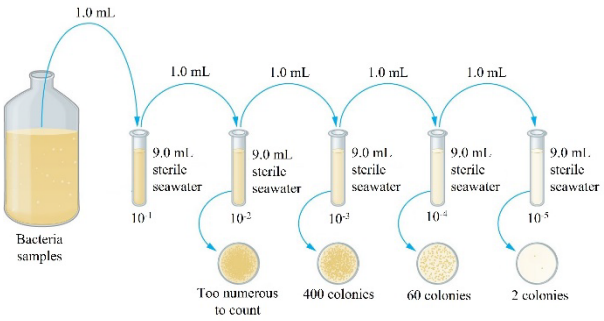

Fig. 1: A dilution factor for bacterial culture.

2.6 Electrochemical measurements

The electrochemical impedance spectroscopy (EIS) and potentiodynamic polarisation curves were executed using a potentiostat (Gamry References 3000). As a reference, a silver/silver chloride (Ag/AgCl) was employed, whereas a platinum rod and a coupon serve as counter electrodes and working electrodes. The EIS attained open circuit potential (OCP) when applied a 10mV signal of sinusoidal voltage with frequencies between 10^{-2} to 10^5 Hz. Setting the scan rate to 0.2 mV/s, the potentiodynamic polarisation curves were calculated by scanning the potential from -250 mV to +350 mV vs OCP. The data received from the polarisation curves and EIS with suitable equivalent circuit models were analysed using the Gamry Echem Analyst.

3. Results and discussion

3.1 Biofilm morphology

FESEM imaginings for SRB biofilms after 72 hours of incubation are shown in Fig. 2 where vibrio and sphere shaped bacteria appear enveloping the entire carbon steel surface. The vibrio shaped bacteria, as spotted in Fig. 2, are typical *Desulfovibrio sp.* SRB cells at sizes around 1.5-2.0 µm[18]. Meanwhile, the sphere or cocci shape bacteria reveal another strain of SRB belonging to the *Desulfococcus multivorans sp.*[19]. In this micrograph, the manifestation of SRB was indicated by a strong scent, seemingly to a decomposed egg. and a display of black VMNI broth. These attributes suggest the decrease of sulfate and development of H_2S and FeS. Previous studies involving SRB discovered a similar result[20].

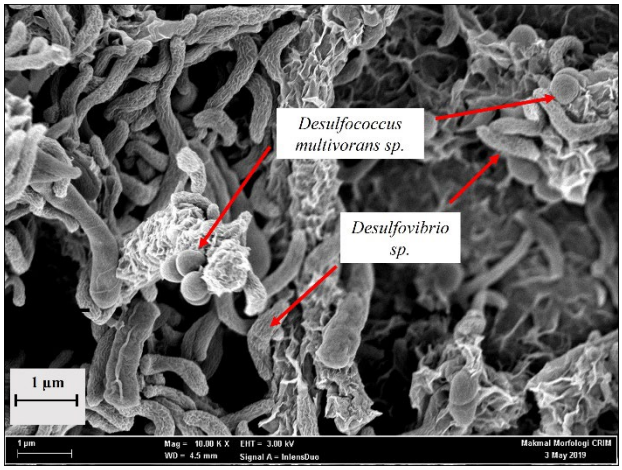

Fig. 2: FESEM image for the SRB biofilm formed in CO_2 – VMNI medium 72 hours incubation at 30ºC.

The biofilm development on the metal surface signifies the onset of MIC. The metal substrate is attached by SRB cells; they soon grow, replicate and generate an extracellular polymeric substance (EPS) resulting a phenomenon termed as biofilm formation. As shown in Fig. 2, the biofilm and MIC products have an inhomogeneous morphology and thickness. The metal substrate could barely be seen in a porous black layer[21]. The substance identical to slimes noticed on the corrosion produces are hypothesised as EPS. The EPS and corrosion products usually take up to 75-95% of biofilms volume, while cells occupy 5-25%.

3.2 The growth process of bacteria

Fig. 3 shows the 30-day development curve of SRB populations in the VMNI medium with CO_2 at 30°C. The SRB growth curve can be divided into four phases: a lag phase (initial phase), an exponential phase, a stationary stage, and a decline phase. Day one to five is the lag phase for SRB. In this phase, the bacterial cells begin to adapt to the environment, and the number of cells is low as the cell is still new to divide. After five to ten days, the growth process of SRB begins to enter the second phase (exponential phase). The highest number of cells can be found in this phase. The number of bacteria increased rapidly and can hypothetically achieve their maximum number[18]. In the second phase, on day ten, the bacterial metabolism occurs at a high rate as a result of rapid cell growth and increased cell numbers. In addition, nutrients as an energy source are consumed to the maximum[22]. As a result of these bacterial cells' metabolism activity, biofilms will form and accelerate the carbon steel surface's corrosion process. The stationary phase of SRB was observed after day ten until day 19. In the third phase, the number of bacteria started to decline and were steadily maintained. After day 19, the numbers of bacteria begins to decrease, indicating a decline in bacterial metabolic activity[23]. In the decline phase, the amount of nutrients that is the carbon source is no longer able to meet the cells' needs. This decline causes bacterial cells to slow down[24].

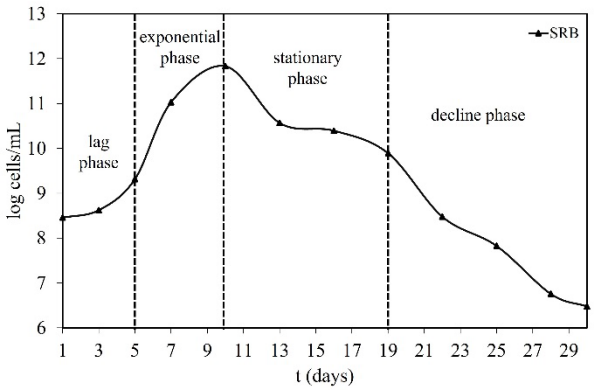

Fig. 3: Growth curves phase of SRB in CO_2 gas flow at 30°C for 30 days.

3.3 Electrochemical impedance spectroscopy (EIS)

The non-destructive electrochemical test known as the electrochemical impedance spectroscopy (EIS), in this study, was adopted to examine electrochemical reactions of MIC on the coupon surface [25]. The EIS measurements were conducted at 30ºC during 14 days of immersion with a continuous CO_2 gas flow. The control conditions are specimens immersed in CO_2 environments without the presence of SRB. Fig. 4 demonstrates the Nyquist diagrams for the steel specimens through a 14-day test with and without SRB in CO_2 environments. The impedance loops of control conditions (Figure 4a), on daily tests, are usually greater than those measured with SRB; more significant readings indicate lesser corrosion occurrence. The impedance loops of specimens without SRB decreased with more time of exposure, indicating that the corrosion has increased over time[26]. In the first four days with the presence of SRB (Figure 4b), the sizes of semicircle increased, but decreased on day seven. On the fourth day, the Nyquist plot diameter attains the highest reading signifying that the presence of SRB may begin to develop biofilms on the surface of the steel[11].

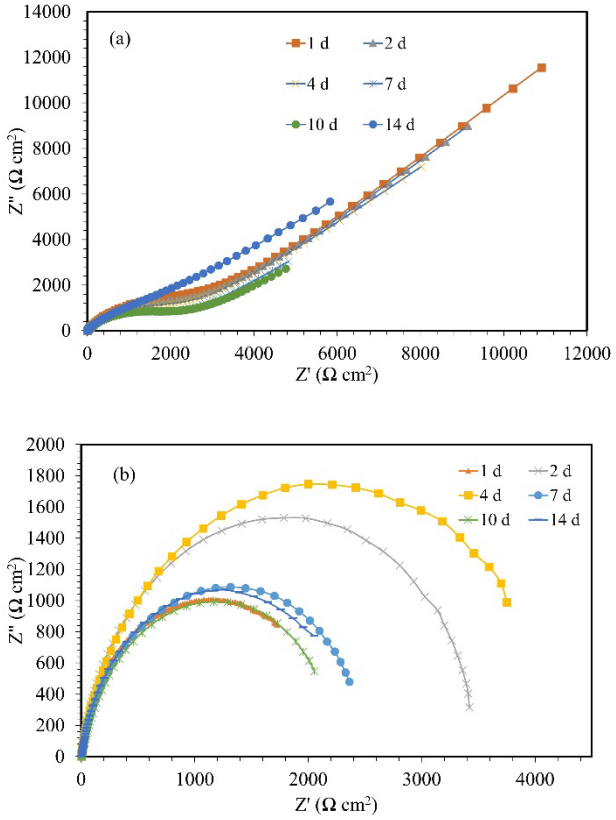

Fig. 4: The Nyquist plot of (a) without and (b) with SRB within a 14-day test.

Fig. 5 illustrates the circuits used to obtain the entire data of EIS in CO_2 environments. Fig. 5a presents the electrical circuit manipulated to tailor the SRB data; whereas, Fig. 5b presents the circuit model without SRB. R_s is the solution resistance, whereas R_f is the resistance, and Q_f is the constant-phase elements of the surface film. On the other hand, R_{ct} is the charge-transfer resistance, Q_{dl} is the double-charge layer's constant-phase element, and W is the Warburg impedance. The circuit capacitance is replaced by the constant phase element (Q) through deliberating the corroded steel specimen's heterogeneity. The Q and Z_q impedances are measured by the following:

$$Z_Q = Y_0^{-1}(j\omega)^{-\alpha} \qquad (2)$$

ω indicates the angular frequency (rads), and Y_0 and α are exponents signifying the specimen deviation from an ideal capacitive behaviour[27].

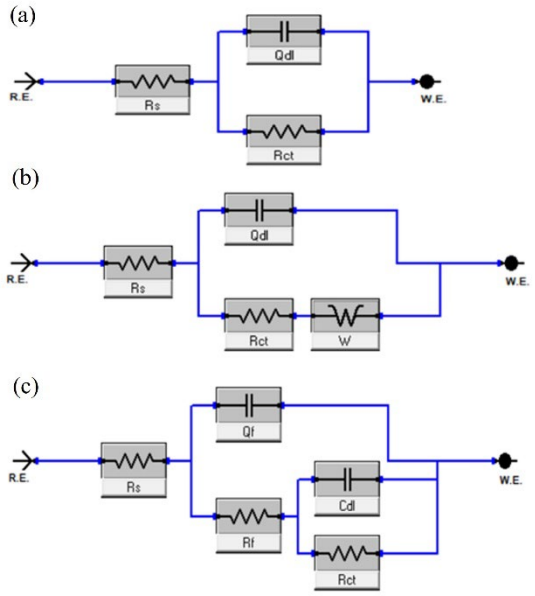

Fig. 5: Electrochemical circuits to design the EIS data: (a) with SRB, (b) and (c) without SRB.

Fig. 6 shows R_p values' time dependence, which was fitted from EIS data for SRB, where the R_p is the outline of R_f and R_{ct}, $R_p = R_f + R_{ct}$. R_p is the inverse proportion of the corrosion value. Generally, a greater R_p reveals a lesser steel corrosion rate. From the data, the R_p readings in the company of SRB are lesser than those without SRB. Such observation conforms that SRB exert severe corrosion effects on carbon steel.

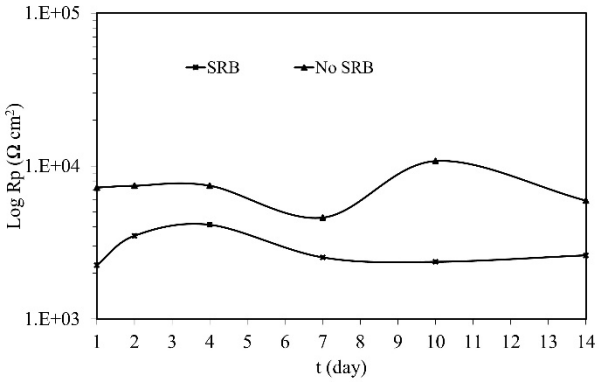

Fig. 6: The changes of R_p values from EIS fitted data with and without SRB in a CO_2 environment.

3.4 Potentiodynamic polarisation

Fig. 7 shows the potentiodynamic polarisation coupon curves for SRB after a 14-day incubation. In the company of SRB, the polarisation curves indicate an accelerated reaction in both anodic and cathodic branches. The E_{corr} reading shifted to the negative direction with SRB indicating an enhanced steel corrosion activity. The corresponding electrochemical fitting parameters were

itemised in Table 1. The corrosion current density (i_{corr}) with SRB at the value of 8.55 x 10^{-6} A cm^{-2} was considerably larger than (i_{corr}) for the control specimen (3.82 x 10^{-6} A cm^{-2}). The value of i_{corr} is proportionate to the steel's corrosion rate[28]. The corrosion rate values obtained from the fitting data indicate that SRB contributes a higher value of 0.397 mm/yr than 0.177 mm/yr recorded by the controlled condition. It is suggested that higher corrosion materialised when the samples were immersed in SRB compared to those without SRB. Thus, the analysis denotes that SRB enhanced the process of corrosion. The curve in Fig. 7 shows a "passive" behaviour at the anodic branch with the presence of the SRB consortium. This behaviour indicates that the potential of the carbon steel significantly increased, pointing to the passivation possibility on the steel surface[29].

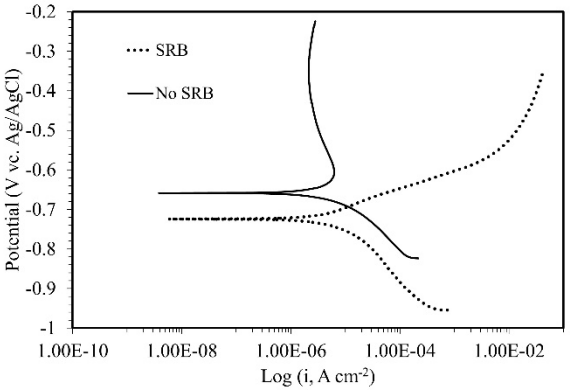

Fig. 7: Potentiodynamic polarisation curves in the with and without SRB after a 14-day test.

Table 1. The measurement of potentiodynamic polarisation data for SRB after a 14-day test under the fitting of electrochemical corrosion parameter.

Bacteria	E_{corr} (V)	I_{corr} (A/cm^2)	Corrosion rate (mm/yr)	Beta a (V/decade)	Beta c (V/decade)
No SRB	-0.659	3.82 x 10^{-6}	0.177	0.2890	0.1400
SRB	-0.724	8.55 x 10^{-6}	0.397	0.0542	0.1132

3.5 Carbon steel's surface morphology

The corrosion surface morphologies for the carbon steel coupons with and without SRB after a 14-day immersion is presented in Fig. 8. In the coupons exposed to the CO_2 environment without SRB (as shown in Figure 8a), the steel surface was enveloped by uniform corrosion. Meanwhile, in the solution containing SRB as depicted through Fig. 8b, a tiny pitting corrosion is spotted. From the evidence gathered, the activity of SRB not just accelerate the corrosion but promotes pitting corrosion. These results could support the data acquired from potentiodynamic polarisation curves indicating the passivity of the steel submerged along with SRB.

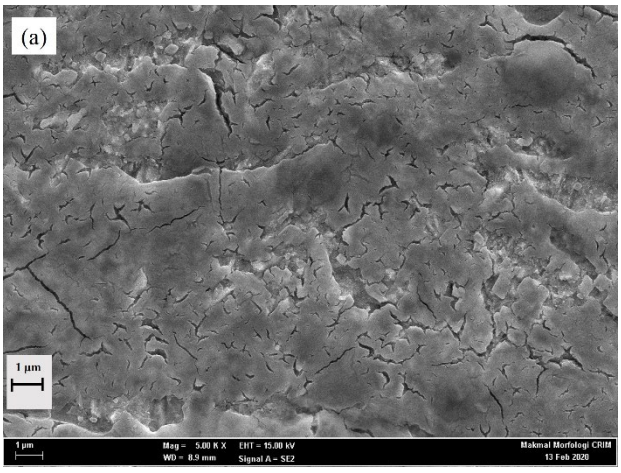

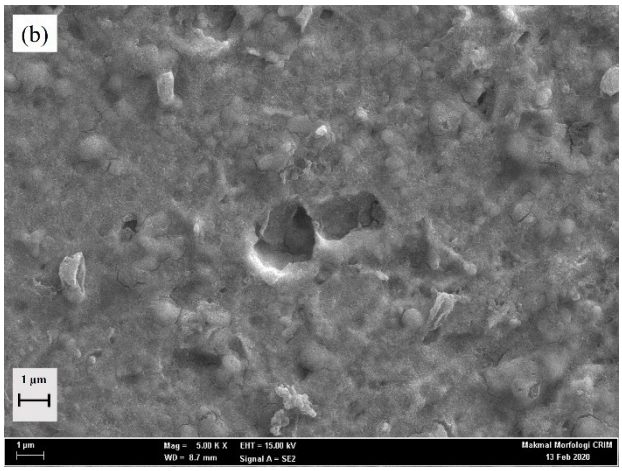

Fig. 8: Corrosion morphology of carbon steel (a) without and (b) with SRB within 14 days of testing.

3.6 Corrosion behaviour of SRB in CO_2 environment

This study exhibits that SRB can thrive in CO_2 environments (Fig. 2 and 3). SRB can utilise the electron supply from CO_2 to grow sessile SRB cells[27]. Consequently, more sessile SRB cells attach themselves onto the steel's surface and contribute to progression of corrosion[30]. The presence of both SRB and CO_2 accelerate the steel corrosion in the solution[22]. Besides contributing to the growth of SRB, CO_2 is able to partake in steel MIC by directly attaining electrons from Fe[31]:

$$4Fe^{2+} + SO_4^{2-} + 5H^+ + 3HCO_3^- \rightarrow$$

$$FeS + 3FeCO_3 + 4H_2O \qquad (3)$$

The acceleration of carbon steel corrosion with SRB in

solutions containing CO_2 gas is shown in the corrosion rate value in Table 1. The existence of SRB substantially stimulates both anodic and cathodic reactions (Figure 7), hence, accumulating corrosion current densities (Table 1).

4.0 Conclusion

Bacteria cell counts from CFU techniques shows that SRB could survive well in CO_2 environments. The FESEM micrograph depicted a distribution of SRB, featuring vibrio and sphere shapes belonging to *Desulfovibrio* sp and *Desulfococcus multivorans* sp. The R_p value from EIS indicates lower values suggesting a higher rate of corrosion. The values of corrosion rate obtained from polarisation fitting data indicate that SRB contribute a higher value of 0.397 mm/yr than the controlled specimen (0.177 mm/yr). It is shown that the presence of SRB, due to MIC, will quicken the corrosion process.

Acknowledgements

The authors would like to acknowledge Ministry of Higher Education, Malaysia and Universiti Kebangsaan Malaysia (FRGS/1/2020/TKO/UKM/02/35) and DNVGL@UKM for encouraging and supporting this research works.

Nomenclature

MIC	Microbiologically Influenced Corrosion
SRB	Sulfate-Reducing Bacteria
EIS	Electrochemical Impedance Spectroscopy
FESEM	Field Emission Scanning Electron Microscopy
CFU	Colony-Forming Unit
R_p	Polarisation resistance
R_s	Solution resistance
R_{ct}	Charge transfer resistance
Q	Constant phase element
Q_{dl}	Double layer
W	Wardburg
Ag/AgCl	Silver/Silver Chloride
OCP	Open Circuit Potential

Greek symbols

ω	angular frequency (rads),

Subscripts

corr	corrosion

References

1) M. Shah, N.R. Abdul Manap, M.T. Mawardi Ayob, N. Yaakob, Z. Embong, and N. Kamil Othman, "EFFECT of ph2s influence on austenitic stainless steel 316l corrosion behaviours in chloride environment / kesan pengaruh tekanan separa gas h2s terhadap tingkah laku kakisan keluli tahan karat 316l di persekitaran klorida," *Malaysian J. Civ. Eng.*, **33** (*2 SE*-) (2021). doi:10.11113/mjce.v33.16697.
2) F. Yulia, S. Marsya, Y. Bobby, Nasruddin, and A. Zulys, "Design and preparation of succinic acid-based metal-organic frameworks for co2 adsorption technology," *Evergreen*, **7** (*4*) 549–554 (2020). doi:10.5109/4150475.
3) A. Wahid, D.R. Mustafida, and Y.A. Husnil, "Exergy analysis of coal-fired power plants in ultra supercritical technology versus integrated gasification combined cycle," *Evergreen*, **7** (*1*) 32–42 (2020). doi:10.5109/2740939.
4) S. Choudhary, A. Sharma, K. Srivastava, H. Purohit, and M. Vats, "Read range optimization of low frequency rfid system in hostile environmental conditions by using rsm approach," *Evergreen*, **7** (*3*) 396–403 (2020). doi:10.5109/4068619.
5) T. Fujisaki, "Evaluation of green paradox: case study of japan," *Evergreen*, **5** (*4*) 26–31 (2018). doi:10.5109/2174855.
6) N.A. Lestari, "Reduction of co2 emission by integrated biomass gasific ation-solid oxide fuel cell combined with heat recovery and in-situ co2 utilization," *Evergreen*, **6** (*3*) 254–261 (2019). doi:10.5109/2349302.
7) S. Guo, L. Xu, L. Zhang, W. Chang, and M. Lu, "Corrosion of alloy steels containing 2 % chromium in co 2 environments," *Corros. Sci.*, **63** 246–258 (2012). doi:10.1016/j.corsci.2012.06.006.
8) N. Ochoa, C. Vega, and P. Nadine, "CO 2 corrosion resistance of carbon steel in relation with microstructure changes b e," **156** 198–205 (2015). doi:10.1016/j.matchemphys.2015.02.047.
9) U. Eduok, M. Khaled, A. Khalil, R. Suleiman, and B. El Ali, "Probing the corrosion inhibiting role of a thermophilic bacillus licheniformis biofilm on steel in a saline axenic culture," *RSC Adv.*, **6** (*22*) 18246–18256 (2016). doi:10.1039/c5ra25381k.
10) S. Maruthamuthu, B.D. Kumar, S. Ramachandran, B. Anandkumar, S. Palanichamy, M. Chandrasekaran, P. Subramanian, and N. Palaniswamy, "Microbial corrosion in petroleum product transporting pipelines," *Ind. Eng. Chem. Res.*, **50** (*13*) 8006–8015 (2011). doi:10.1021/ie1023707.
11) H. Liu, C. Fu, T. Gu, G. Zhang, Y. Lv, H. Wang, and H. Liu, "Corrosion behavior of carbon steel in the presence of sulfate reducing bacteria and iron oxidizing bacteria cultured in oilfield produced water," *Corros. Sci.*, **100** 484–495 (2015). doi:10.1016/j.corsci.2015.08.023.
12) H. Castaneda, and X.D. Benetton, "SRB-biofilm influence in active corrosion sites formed at the steel-

electrolyte interface when exposed to artificial seawater conditions," *Corros. Sci.*, **50** (*4*) 1169–1183 (2008). doi:10.1016/j.corsci.2007.11.032.

13) M.S. De Paula, M.M.M. Gonçalves, M.A. da C. Rola, D.J. Maciel, L.F. De Senna, and D.C.B. Do Lago, "Carbon steel corrosion induced by sulphate-reducing bacteria in artificial seawater: electrochemical and morphological characterizations," *Rev. Mater.*, **21** (*4*) 987–995 (2016). doi:10.1590/S1517-707620160004.0091.
14) N. Angie, E.M. Tokit, N.A. Rahman, F. Al Zahrah Mohamad Saat, F.S. Anuar, and N.M.M. Mitan, "A preliminary conceptual design approach of food waste composter design," *Evergreen*, **8** (*2*) 397–407 (2021). doi:10.5109/4480721.
15) M.N. Idris, N.A. Mahat, N.K. Othman, and F.K. Shahrani, "Anaerobic bacteria treatment by benzyl dimethyl (2-hidroxyethyl) ammonium chloride for carbon steel pipeline system," **2** 12–17 (2017).
16) V. Zinkevich, I. Bogdarina, H. Kang, M.A.W. Hill, R. Tapper, and I.B. Beech, "Characterisation of exopolymers produced by different isolates of marine sulphate-reducing bacteria," *Int. Biodeterior. Biodegrad.*, **37** (*3–4*) 163–172 (1996). doi:10.1016/s0964-8305(96)00025-x.
17) S. Maruthamuthu, S. Mohanan, A. Rajasekar, N. Muthukumar, S. Ponmarippan, P. Subramanian, and N. Palaniswamy, "Role of corrosion inhibitor on bacterial corrosion in petroleum product pipelines," *Indian J. Chem. Technol.*, **12** (*5*) 567–575 (2005).
18) A. Abdullah, N. Yahaya, M.N. Norhazilan, and R.M. Rasol, "Microbial corrosion of api 5l x-70 carbon steel by atcc 7757 and consortium of sulfate-reducing bacteria," *J. Chem.*, **2014** (2014). doi:10.1155/2014/130345.
19) P.F. Almeida, E.B. Carvalho, E.R. Souza, A.S. Carvalho, C.H.T.P. Silva, C.A. Taft, M. Calmon, and R. De Janeiro, "Overview of sulfate-reducing bacteria and strategies to control biosulfide generation in oil waters," *Mod. Biotechnol. Med. Chem. Ind.*, **661** (*2*) 1–15 (2006).
20) F.K. Sahrani, Z. Ibrahim, A. Yahya, and M. Aziz, "Isolation and identification of marine sulphate-reducing bacteria, desulfovibrio sp. and citrobacter freundii from pasir gudang, malaysia," *Sains Malaysiana*, **37** (*4*) 365–371 (2008).
21) F.M. Al Abbas, R. Bhola, J.R. Spear, D.L. Olson, and B. Mishra, "Electrochemical characterization of microbiologically influenced corrosion on linepipe steel exposed to facultative anaerobic desulfovibrio sp.," *Int. J. Electrochem. Sci.*, **8** (*1*) 859–871 (2013).
22) A.J. Wikieł, I. Datsenko, M. Vera, and W. Sand, "Impact of desulfovibrio alaskensis biofilms on corrosion behaviour of carbon steel in marine environment," *Bioelectrochemistry*, **97** 52–60 (2014). doi:10.1016/j.bioelechem.2013.09.008.
23) A.E. Zakaria, H.M. Gebreil, and N.M. Abdelaal, "Control of microbiologically induced corrosion in petroleum industry using various preventive strategies," *Arab J. Nucl. Sci. Appl.*, **45** (*2*) 460–478 (2012).
24) N.A. Mahat, N.K. Othman, F.K. Sahrani, and M.N. Idris, "Inhibition of consortium sulfate reducing bacteria from crude oil for carbon steel protection," *Sains Malaysiana*, **44** (*11*) 1587–1591 (2015).
25) R. Jia, D. Yang, D. Xu, and T. Gu, "Anaerobic corrosion of 304 stainless steel caused by the pseudomonas aeruginosa biofilm," *Front. Microbiol.*, **8** (*NOV*) 1–9 (2017). doi:10.3389/fmicb.2017.02335.
26) P. Bai, S. Zheng, and C. Chen, "Electrochemical characteristics of the early corrosion stages of api x52 steel exposed to h2s environments," *Mater. Chem. Phys.*, **149** 295–301 (2015). doi:10.1016/j.matchemphys.2014.10.020.
27) H. Liu, and Y.F. Cheng, "Mechanistic aspects of microbially influenced corrosion of x52 pipeline steel in a thin layer of soil solution containing sulphate-reducing bacteria under various gassing conditions," *Corros. Sci.*, **133** (*October 2017*) 178–189 (2018). doi:10.1016/j.corsci.2018.01.029.
28) H. Liu, G. Meng, W. Li, T. Gu, and H. Liu, "Microbiologically influenced corrosion of carbon steel beneath a deposit in co2-saturated formation water containing desulfotomaculum nigrificans," *Front. Microbiol.*, **10** (*JUN*) 1–13 (2019). doi:10.3389/fmicb.2019.01298.
29) T. Wu, C. Sun, J. Xu, M. Yan, F. Yin, and W. Ke, "A study on bacteria-assisted cracking of x80 pipeline steel in soil environment," *Corros. Eng. Sci. Technol.*, **53** (*4*) 265–275 (2018). doi:10.1080/1478422X.2018.1456633.
30) J. Wang, Z. Liu, S. Bai, J. Cao, J. Zhao, and D. Zeng, "Combined effect of ag and mg additions on localized corrosion behavior of al-cu alloys with high cu content," *J. Mater. Eng. Perform.*, **29** (*9*) 6108–6117 (2020). doi:10.1007/s11665-020-05072-6.
31) D. Enning, and J. Garrelfs, "Corrosion of iron by sulfate-reducing bacteria: new views of an old problem," *Appl. Environ. Microbiol.*, **80** (*4*) 1226–1236 (2014). doi:10.1128/AEM.02848-13.